Use of Two Singular Point Finite Elements in the Analysis of Kinked Cracks

B. K. DUTTA*, A. KAKODKAR*, and S. K. MAITI**
**Reactor Engineering Division, Bhabha Atomic Research Centre, Bombay 400 085, India*
***Indian Institute of Technology, Bombay 400 076, India*

ABSTRACT

An element formulation is suggested to obtain variable order singularities simultaneously at two corner nodes of a side of a 4-noded quadrilateral. The element is useful for modelling a kinked crack with small kink length. The performance of the element is demonstrated by considering three different examples of kinked cracks. The path independency and the influence of mesh refinement on the computation of J integral are also examined.

KEYWORDS

Kinked cracks, Two point singularity element, Finite element analysis of kinked cracks.

INTRODUCTION

Under mixed mode loading a crack leads to an out-of-plane extension and hence kinking. In stable crack propagation studies under this type of loading, one has to deal with kinked cracks. For a small kink length, an analysis of the problem is difficult due to the existence of two singular points at a close distance. At the crack tip, there is a square root singularity, whereas at the knee the order of singularity depends on the kink angle (Williams, 1952). One obvious strategy is to use of wellknown quarter point elements (Barsoum, 1976) at the crack tip for the simulation of square root singularity and the 3-noded variable order triangular singularity elements (Tracey and Cook, 1977) at the knee. The two elements must be separated by a number of conventional elements. This will usually lead to a large number of elements and nodes and hence more computational cost. One alternative strategy is to use one single element to cover the whole kink length. This provided motivation for the development

of the two singular point (TSP) finite elements.

We had some success in developing such an element (Dutta et al., 1988). In this paper the element formulation is presented briefly. The element has been used here to analyse three different kinked crack problems. In the first example, a kinked crack under tensile loading, the path independency and the effect of mesh refinement surrounding the TSP element on J computation are examined. In the last two examples, a four point bend and a three point bend specimen configurations, the strain energy release rate is calculated along various contours around the crack tip and their average values are compared with a first order analytical solution.

ELEMENT FORMULATION

Consider a 4-noded quadrilateral element as shown in Fig. 1a. The element can be mapped into a square in the conventional (ξ,η) system of natural coordinates (Fig. 1b). Consider now a local coordinate system (ρ_1,ρ_2) defined by

$$\rho_1 = (2+\xi+\eta)/4 \quad \text{and} \quad \rho_2 = (2-\xi+\eta)/4 \tag{1}$$

In this (ρ_1,ρ_2) system the coordinates of the four corner nodes are shown in Fig.1b . The shape function N_i associated with node i can be written in terms of equations of two element sides which are not passing through this node. For example, the shape function associated with node 1 can be written as

$$N_1 = (+\rho_1 - \rho_2 - 0.5)(\rho_1 + \rho_2 - 1.5) \tag{2}$$

Note that the first expression is the equation of side 2-3, and the second expression is the equation for side 3-4.

To facilitate an exponential variation of the field variable in the directions ρ_1 and ρ_2, a geometric mapping is done. In this (α,β) system, where $\alpha = \rho_1^{\lambda_1}$ and $\beta = \rho_2^{\lambda_2}$, the element is shown in Fig. 1c. The four displacement shape functions can be written from the equations of four sides of the element in this coordinate system. These shape functions are shown below.

$$\begin{aligned}
N_1 &= C_1(A_{23}\rho_1^{\lambda_1}+\rho_2^{\lambda_2}+B_{23})\ (A_{34}\rho_1^{\lambda_1}+\rho_2^{\lambda_2}+B_{34})\\
N_2 &= C_2(A_{34}\rho_1^{\lambda_1}+\rho_2^{\lambda_2}+B_{34})\ (A_{41}\rho_1^{\lambda_1}+\rho_2^{\lambda_2}+B_{41})\\
N_3 &= C_3(A_{41}\rho_1^{\lambda_1}+\rho_2^{\lambda_2}+B_{41})\ (A_{12}\rho_1^{\lambda_1}+\rho_2^{\lambda_2}+B_{12})\\
N_4 &= C_4(A_{12}\rho_1^{\lambda_1}+\rho_2^{\lambda_2}+B_{12})\ (A_{23}\rho_1^{\lambda_1}+\rho_2^{\lambda_2}+B_{23})
\end{aligned} \tag{3}$$

where $A_{12} = 2^{\lambda_1}/2^{\lambda_2}$; $B_{12} = -1/2^{\lambda_2}$

$C_1 = \{2^{2\lambda_2}(1-2^{\lambda_1})^2\}/\{2^{2\lambda_1}(1-2^{\lambda_2})\}$

$A_{23} = 2^{\lambda_1}/\{2^{\lambda_2}(1-2^{\lambda_1})\}$

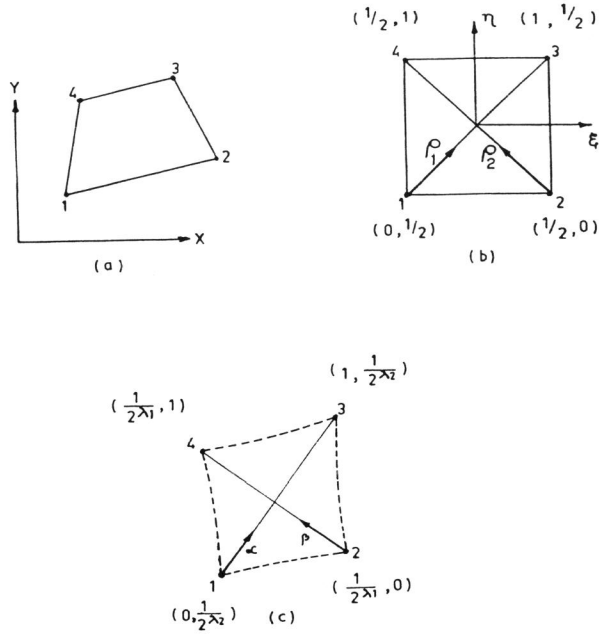

Fig.1. Illustration used to derive the displacement shape functions for a TSP element

$$\begin{aligned}
B_{23} &= 1/\{2^{\lambda_2}(2^{\lambda_1}-1)\}\\
C_2 &= 1\\
A_{34} &= \{2^{\lambda_1}(1-2^{\lambda_2})\}/\{2^{\lambda_2}(1-2^{\lambda_1})\}\\
B_{34} &= \{2^{\lambda_1}(2^{\lambda_2}-1)\}/\{2^{\lambda_2}(1-2^{\lambda_1})\} - 1/2^{\lambda_2}\\
C_3 &= 2^{2\lambda_2}/\{2^{2\lambda_1}(1-2^{\lambda_2})\}\\
A_{41} &= 2^{\lambda_1}(1-2^{\lambda_2})/2^{\lambda_2}\\
B_{41} &= -1/2^{\lambda_2}\\
C_4 &= 1
\end{aligned} \tag{4}$$

These shape functions satisfy the completeness requirement only when $\lambda_1 = \lambda_2 = 1$. If the element displacement field is interpolated using these shape functions, i.e.

$$u = \sum_1^4 N_i\, u_i \quad \text{and} \quad v = \sum_1^4 N_i\, v_i ,$$

a TSP element is obtained. Arbitrary singularities can be got by assigning appropriate values to λ_1 and λ_2. The order of singularities are $-1+\lambda_1$ at $\rho_1 \to 0$ and $-1+\lambda_2$ at $\rho_2 \to 0$. The

derivatives of the shape functions in (ξ,η) coordinates can be found out by using the suitable Jacobian matrix relating (ρ_1,ρ_2) and (ξ,η) systems. It may be noted here that (ρ_1,ρ_2) is linearly related to (ξ,η). In turn, (ξ,η) is linearly related to (x,y). The derivatives of shape function (N_i's) retain the order of singularity even when any of the two corner nodes are approached alongan arbitrary ray emanating from it.

To improve the completeness characteristics, the element displacement field can be written

$$u = \sum_1^5 N_i\, u_i \quad \text{and} \quad v = \sum_1^5 N_i\, v_i$$

where

$$N_5 = \rho_1^{\lambda 1}(1-\rho_1^{\lambda 1})\ \rho_2^{\lambda 2}(1-\rho_2^{\lambda 2})\ C_\lambda(1-C_v)$$

where $C_v = \sum N_i$ at (0.5, 0.5), $i = 1,4$ and

$$C_\lambda = 2^{2(\lambda_1+\lambda_2)}/\{(2^{\lambda 1}-1)\ (2^{\lambda 2}-1)\}$$

This modification gives rise to $\sum_1^5 N_i = 1$ at the four corner nodes, centre of the element and also along the two axes (ρ_1,ρ_2). The u_5 and v_5, which can be thought of as nodeless variables, are associated with the element only. They can be condensed at the element level before the assembly of element stiffness matrices.

CASE STUDIES

Performance of the element is illustrated by presenting three case studies. The first case deals with the double edge kinked crack under tension (Fig. 2a). The study is done for the kink angles of 15°, 30°, 45° and 60°. This case mainly concerns with the effect of mesh refinement surrounding the TSP element on the J-integral computation. Fig. 2 also shows the different discretization schemes for the regions near to kink and away from kink for a kink angle of 45°. Three mesh arrangements are considered. The first arrangement is obtained by combining 2b and 2d. The second and the third correspond to combinations of 2c and 2d, and 2c and 2e respectively. For other kink angles the relevant nodal coordinates near to kink are suitably modified. J-integrals along three different contours around the crack tip are calculated. Table 1 shows these values for all mesh patterns. Their average values for various kink angles are compared with a first order analytical solution (Cottrell and Rice, 1980). The path independence of J and marginal effect of mesh refinement on the J computation are seen from these results. A crack of this configuration will extend in an arbitrary angle with the kink. Similarly, a crack under mixed mode will extend out-of-plane. Further studies on any of this type of extended crack will call for a multiple use of the TSP element.

The second example is that of a 4-point bend specimen configuration (Fig. 3a). The study is done for θ in the range 15° to 90° in steps of 15°. The mesh arrangement is similar to the discretization schemes shown in Fig. 2b and 2d. The J-integral was

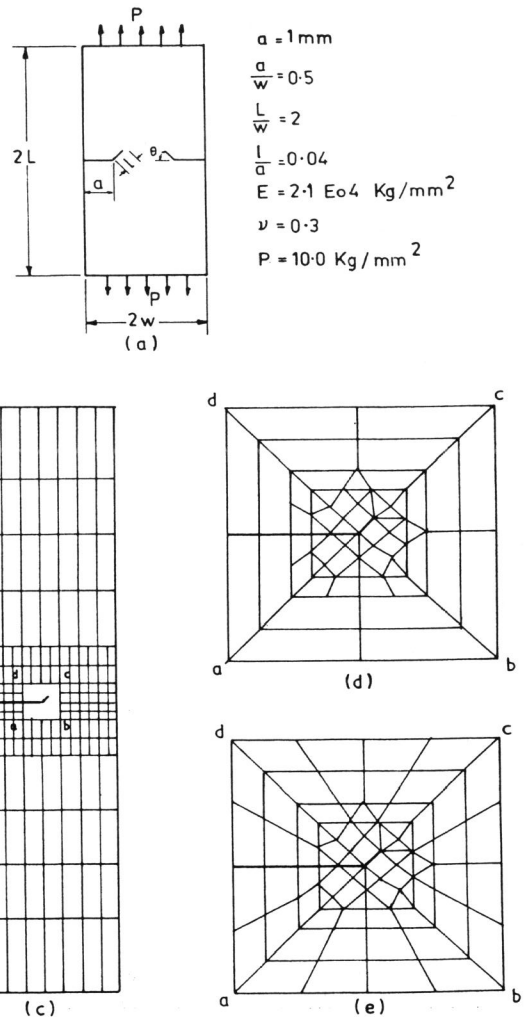

Fig. 2 (a) Double edge kinked crack in a tension strip.
(b),(c) Discretization schemes away from kink.
(d),(e) Discretization schemes near to kink.

computed using three different contours around the crack tip. The average of computed J values are compared with the first order analytical solution (Cottrell and Rice, 1980) in Fig. 3b. The agreement is good.

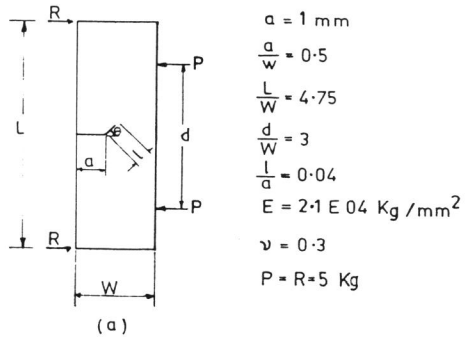

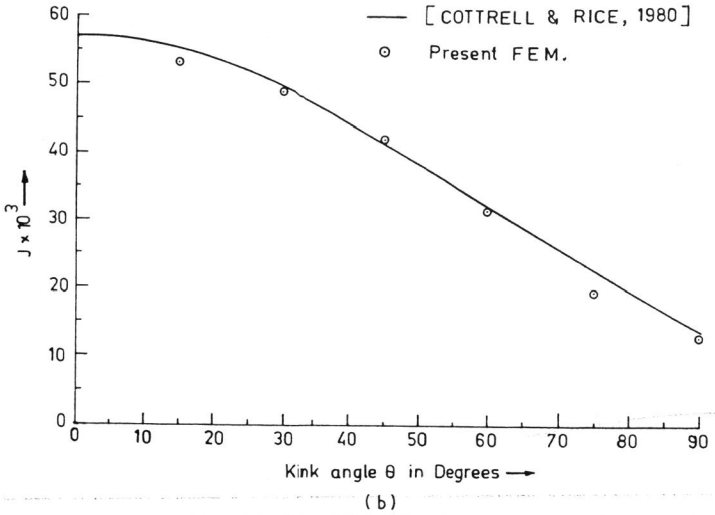

Fig. 3(a) Single edge kinked crack under four point bending.
(b) Comparism of computed J with an analytical solution.

The last example consists of a 3-point bend specimen configuration (Fig. 4a). The study was done in this case along the lines similar to that of 4-point bend specimen. The average of computed J values are compared with the analytical solution in Fig. 4b. The agreement is again good.

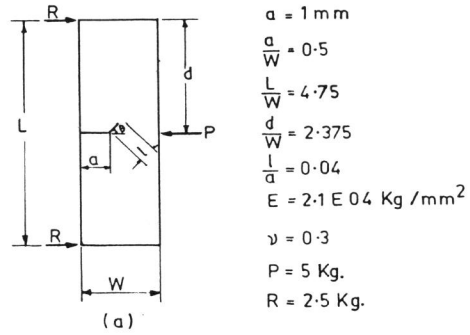

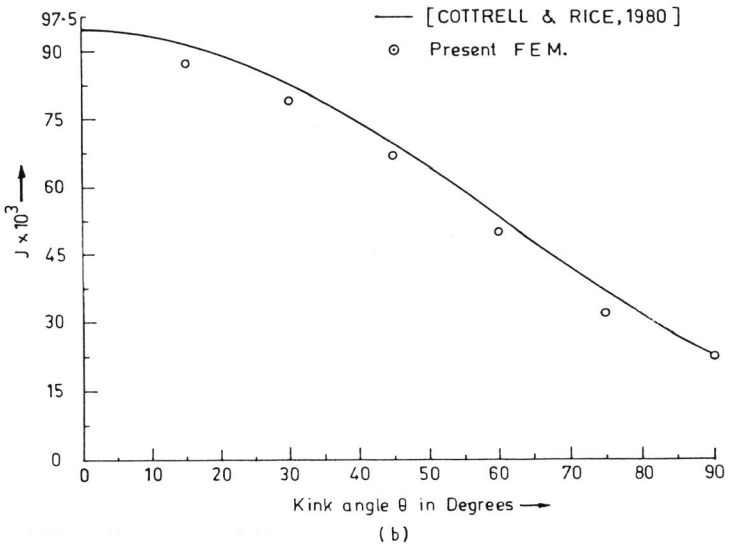

Fig. 4 (a) Single edge kinked crack under three point bending.
(b) Comparison of computed J with an analytical solution.

CONCLUSION

We have presented an approach for the inclusion of more than one point of singularity in a single element. These case studies demonstrate that the approach is quite feasible. In all the case studies the computed values of J compare closely with

Table 1. Effect of mesh refinement on J computation in the case of double edge kinked crack problem

θ	Cottrell and Rice (1980)	Mesh arrangement-1 (No. of elements = 152 No.of nodes=172)		Mesh arrangement-2 (No. of elements = 236 No.of nodes=275)		Mesh arrangement-3 (No. of elements = 256 No.of nodes=287)	
		J along three contours	J-average	J along three contours	J-average	J along three contours	J-average
		0.01933		0.01924		0.01943	
15°	0.019858	0.01885	0.01948	0.01875	0.01938	0.01920	0.01962
		0.02026		0.02017		0.02025	
		0.01746		0.01737		0.01762	
30°	0.01789	0.01736	0.01774	0.01725	0.01764	0.01762	0.01787
		0.01840		0.01831		0.01838	
		0.01524		0.01509		0.01562	
45°	0.01497	0.01509	0.01529	0.01493	0.01514	0.01548	0.01556
		0.01555		0.01540		0.01558	
		0.01156		0.01114		0.01180	
60°	0.01156	0.01157	0.01163	0.01114	0.01120	0.01176	0.01175
		0.01177		0.01134		0.01169	

first order analytical solution due to Cottrell and Rice (1980). In the first example path independence of J and marginal effect of mesh refinement on J computation are also demonstrated.

REFERENCES

Barsoum, R.S. (1976). On the use of isoparametric finite elements in linear fracture mechanics. Int. J. Num. Meth. Engng., 10, 25-37.

Cottrell, B. and J.R. Rice (1980). Slightly curved or kinked cracks. Int. J. Fract., 16, 155-169.

Dutta, B.K., S.K. Maiti and A. Kakodkar (1988). Two singular point finite elements in the analysis of kinked cracks. Communicated to Int. Jl. of Comp. Mech.

Tracey, D.M. and T.S. Cook (1977). Analysis of power type singularities using finite elements. Int. J. Num. Meth. Engng., 11, 1225-1233.

Williams, M.L. (1952). Stress singularities resulting from various boundary conditions in angular corners of plates in extension. J. Appl. Mech., 19, Trans. ASME, 74, Series E, 526-528.